LAWRENCE
LIVERMORE
NATIONAL
LABORATORY

LLNL-CONF-415592

Using collective x-ray Thomson scattering to measure temperature and density of warm dense matter

T. Doeppner, P. F. Davis, A. L, Kritcher, O. L. Landen, H. J. Lee, S. P Regan, S.H. Glenzer

August 13, 2009

SPIE Optics and Photonics Conference
San Diego, CA, United States
August 2, 2009 through August 6, 2009

Disclaimer

Using collective x-ray Thomson scattering to measure temperature and density of warm dense matter

T. Döppner[a], P.F. Davis[b], A.L. Kritcher[b], O.L. Landen[a], H.J. Lee[b], S.P. Regan[c], S.H. Glenzer[a]

[a]Lawrence Livermore National Laboratory, P.O. Box 808, Livermore, CA 94551, USA;
[b]University of California, Berkeley, CA 94720, USA;
[c]Laboratory for Laser Energetics, University of Rochester, 250 East River Road, Rochester, New York 14623-1299, USA

ABSTRACT

Collective x-ray Thomson scattering allows measuring plasmons, i.e electron plasma oscillations (Langmuir waves). This is manifest in the appearance of spectrally up- and down-shifted spectral features in addition to the Rayleigh signal. The ratio of the up- and down-shifted signals is directly related to detailed balance, allowing to determine the plasma temperature from first principles. The spectral shift of the plasmon signals is sensitive to temperature and electron density. We discuss the experimental considerations that have to be fulfilled to observe plasmon signals with x-ray Thomson scattering. As an example, we describe an experiment that used the Cl Ly-α x-ray line at 2.96 keV to measure collective Thomson scattering from solid beryllium, isochorically heated to 18 eV. Since temperature measurement based on detailed balance is based on first principles, this method is important to validate models that, for example, calculate the static ion-ion structure factor $S_{ii}(k)$.

Keywords: Warm dense matter, Plasma diagnostic, Thomson scattering, Plasmons

1. INTRODUCTION

Accurate characterization of warm dense matter is important for high energy density physics experiments in general,[1] and for inertial confinement fusion[2] and astrophysical problems in particular. Warm dense matter is challenging to describe theoretically, since coupling becomes important. It can be characterized by the fact that the potential energy of the interaction between electrons and nuclei and the kinetic energy of electrons are of roughly the same magnitude. Plasmas in this regime are typically at solid density and above with temperatures of order few eV. They can no longer be characterized with traditional spectroscopy techniques based on optical Thomson scattering because they are opaque to visible light.

Only recently, intense lasers have become available that provide powerful x-ray sources able to penetrate solid density matter. This allowed to extend the concept of spectrally resolved Thomson scattering to higher photon energies up into the x-ray regime, for a recent review see Ref.[3] For example, the Omega laser facility at the Laboratory for Laser Energetics in Rochester provides 60 beams with up to 500 J per pulse that can be sent to target creating an intense and spectrally narrow x-ray probe that fulfills the stringent requirements for single shot experiments. The Omega laser was used to demonstrate x–ray Thomson scattering (XRTS) studying isochorically heated beryllium.[4,5] Meanwhile XRTS has been successfully demonstrated on a number of medium sized laser facilities.[1,6]

Free Electron Lasers (FEL) are very promising x-ray sources due to their high brilliance, high repetition rate, and short pulse length. First Thomson scattering experiments have been demonstrated at the Free Electron Laser in Hamburg (FLASH), probing near solid-density hydrogen with 92 eV VUV radiation.[7] Future experiments will utilize FEL radiation up to multiple keV photon energies at the Linac Coherent Light Source (LCLS), Stanford, and at the X-FEL, Hamburg.

Corresponding author: Tilo Döppner, E-mail: doeppner1@llnl.gov

X-ray Thomson scattering allows to accurately measure electron temperature and density in dense matter. Besides being a valuable plasma diagnostic it can be utilized to validate radiation hydrodynamic codes by, for example, testing their predictions for shock-timing.[1,8] The latter experiments utilized coalescing shocks to shock-compress matter reaching electron densities on order of $n_e = 10^{24}$ cm^{-3}. In addition to demonstrating the diagnostic capability for future studies, e.g., on the National Ignition Facility, present experiments address fundamental questions concerning the physical processes that effect the equation of state in dense matter, the theory of structure factors, and the role of collisions in warm dense matter.

Besides plasma conditions and x-ray probe energy, the design of the scattering geometry determines whether the experiment will probe the collective or non-collective regime. The collectivity parameter

$$\alpha = \frac{1}{k\lambda_{scr}} \tag{1}$$

allows to discriminate between these two regimes, with k the momentum transfer in the scattering process and λ_{scr} the screening length. For small energy transfers of incident x-ray energy to the electrons the magnitude of the scattering vector, $\mathbf{k}$, can be approximated by

$$k = |\mathbf{k}| = 4\pi \frac{E_0}{hc} \sin(\theta/2) \tag{2}$$

where E_0 the photon energy, and θ the scattering angle. The screening length λ_{scr} becomes the Thomas-Fermi length λ_{TF} in a degenerate plasma, and the Debye length λ_D

$$\lambda_D = \sqrt{\frac{\varepsilon_o k_B T_e}{n_e e^2}} \tag{3}$$

in case of a classical plasma, with T_e the electron temperature and n_e the electron density. In between, for weakly-degenerate plasmas, calculating the Debye length at an effective temperature T_{eff} results in a smooth interpolation between λ_D and λ_{TF}.

For $\alpha < 1$, usually obtained experimentally by observation at large scattering angles, the plasma is probed in the non–collective scattering regime, i.e. the scattering is sensitive to the motion of individual electrons. This results in an inelastically scattered Compton feature that is down-shifted in energy, and Doppler-broadened due the velocity distribution of the electrons.[4] In degenerate plasmas the Compton feature has a parabolic shape. Its width is proportional to square root of the Fermi–energy and thus the cube root of electron density n_e. On the other hand, in slightly degenerate and non-degenerate plasmas, the low-energy slope of the Compton feature allows to infer the the plasma temperature.

Here, we will concentrate on the collective scattering case, which is characterized by $\alpha > 1$. It is generally realized in a forward scattering geometry, allowing to observe collective electron density oscillations, i.e., plasmons.[5] The scattering spectrum is sensitive to the electron temperature in several ways. Previously it was demonstrated, that the temperature can be determined from the shape of the down-shifted plasmon signal.[5] To accomplish this, the spectrum was modeled within the Born approximation, including electron-ion collisions using a Mermin ansatz. However, this method relies on theoretical models and is in a regime where collisions are important. A more rigorous method is based on detailed balance,[3,9–11] i.e. the ratio of the up–shifted to the down–shifted plasmon signals:

$$\frac{S(-\mathbf{k}, -\omega)}{S(\mathbf{k}, \omega)} = \exp\left(-\frac{\hbar\omega}{k_B T}\right) \tag{4}$$

here $S(\mathbf{k}, \omega)$ is the dynamic structure factor, which is proportional to the inelastically scattered x–ray signal, $\hbar\omega$ is the energy transfer of the scattered photons, k_B the Boltzmann constant, and T is the equilibrium temperature of the system. This relation is valid when the system is in thermal equilibrium, so that no other assumptions are required. Thus, the detailed balance equation results from the two matrix elements for the transition between two states by electron-photon interaction being equal while quantum levels are occupied according to the relationship imposed by thermodynamic equilibrium. This provides a very powerful tool for the measurement of temperature, which depends only on the principle of detailed balance.

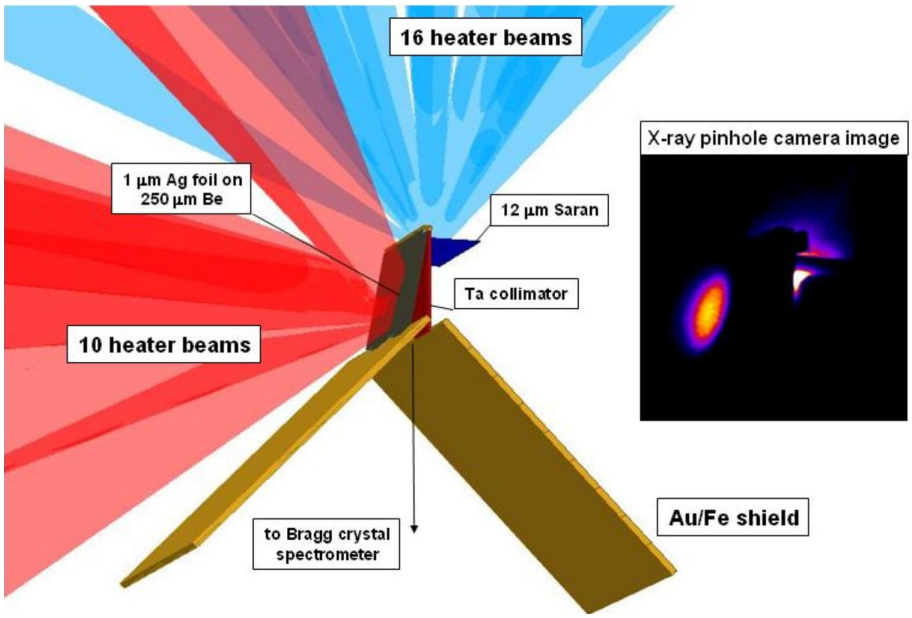

Figure 1. Schematic of the experimental setup. 10 heater beams generate Ag L-shell x rays that isochorically heat a 250 μm thick beryllium foil. 16 probe beams, delayed by 0.9 ns, create the Cl Ly-α x-ray probe at 2.96 keV to measure the plasma conditions. An x-ray pinhole camera records the time-integrated continuum emission which clearly shows the smooth drive beam spot.

Another route to measure the plasma temperature is to exploit the sensitivity of the static ion-ion structure factor $S_{ii}(k)$ on ion temperature T_i. Experimentally, the strength of the nearly elastic Rayleigh feature measures[12,13]

$$W_R(k) = |f_I(k) + q(k)|^2 \, S_{ii}(k), \tag{5}$$

where $f_I(k)$ is the ionic form factor describing the tightly bound electrons, and $q(k)$ the number of free and loosely bound electrons that follow the motion of the ions. In principle, the temperature can be inferred from the ratio of the Rayleigh feature to the spectrally red-shifted plasmon signal. However, this approach requires a correct theoretical model for the static ion-ion structure factor $S_{ii}(k)$, and knowledge of $f_I(q)$ and $q(k)$. Calculations of $S_{ii}(k)$ are currently a topic of active research.[14–16] Once these models have been validated, for example by measurements based on detailed balance, the strength of the Rayleigh feature will allow to reliably infer plasma temperatures.

In Section 2 we describe an experiment that fulfills the requirements on plasma parameters and scattering geometry to observe collective x-ray Thomson scattering. A sufficiently high plasma temperature allows to observe up-shifted plasmon signals. Section 3 discusses the sensitivity of the plasmon signals on electron temperature and electron density, and gives an outlook for future experiments.

2. EXPERIMENTAL OBSERVATION OF COLLECTIVE X-RAY THOMSON SCATTERING

To illustrate the principle of detailed balance, in this section we describe a collective scattering experiment that reached sufficiently high temperatures to observe an up-shifted plasmon signal. The experiment was performed at the Omega laser facility at the Laboratory for Laser Energetics at the University of Rochester. Fig. 1 shows a schematic of the target and the laser beam configuration. To isochorically heat a 250 μm thick Be foil with Ag L-shell radiation, 10 drive beams with a total energy of 4.7 kJ at 351 nm in a 1 ns pulse width were incident on a 1 μm silver foil glued to the Be. Distributed phase plates (DPP, type SG4) were used to achieve a smooth beam spot with a diameter of 800 μm yielding a drive intensity of $7{\times}10^{14}$ W cm^{-2}. To generate the Cl Ly-α x-ray probe at 2.96 keV, 16 beams with a total energy of 7.4 kJ at 351 nm were focused nominally to a 150 μm

spot on a 12 μm Saran foil, yielding an intensity of 3.6×10^{16} W cm^{-2}. The x–ray photons are collimated by a 50 μm thick, rectangular Ta pinhole in front of the Be which defines the scattering angle to 40°. In total, the solid angle of the x-ray source that reaches the heated beryllium foil amounts to 0.2 sr. In the horizontal axis the pinhole width is 600 μm, matched to the size of the drive beam spot, and allowing to only probe the heated region of the beryllium. In the vertical axis the pinhole width, perpendicular to the propagation of the x-ray probe, is 180 μm, restricting the range of scattering angles to $40 \pm 5°$. This is necessary to prevent the blurring of the scattering signal by a too broad range of scattering vectors k.

Both the backlighter performance and the Ag L–shell emission are monitored by a streaked crystal spectrometer. The main contribution to the Ag foil emission stems from 3d–2p transitions between 3.2 and 3.6 keV. No significant Ag plasma emission is observed in the energy range of the x-ray source line used for the Thomson scattering measurement. In addition, the L-shell emission turns off promptly at the end of the heater beams duration. This allows us to probe the plasma conditions very close to the end of the heater beams when the highest plasma temperatures can be expected. In contrast, the Cl K-line emission lasts considerably beyond the end of the probe pulse. The strongest emission observed by the monitor spectrometer is for the Cl Ly-α line. Besides the Cl Ly-α line a satellite, down–shifted by 30 eV, is emitted. By varying the spot size of the backlighter beams we optimized both the conversion efficiency into Cl Ly-α, and minimized the strength of the red–shifted satellite with respect to the main Cl Ly-α line. At intensities of 1.8×10^{16} W cm^{-2} we measured a contrast ratio of 7.6. By increasing the intensity to 3.2×10^{16} W cm^{-2} the contrast improved to 11.2 while the conversion efficiency stayed almost constant. From the streaked spectra it is evident that both the Cl Ly-α emission and the probe line to satellite contrast do not change considerably for the duration of the backlighter beams.

On the other hand, the undiffracted background recorded on the main scattering spectrometer significantly changes with time, and clearly decreases toward the end of the backlighter pulse. Thus, to achieve a good signal–to–noise ratio, the detector is gated late in the probe pulse. Due to the 250 μm mean free path at 3 keV, the x-ray photons scatter predominantly from a 40 μm-deep Be region on the undriven side. An 11° tilt is introduced so scattered 3 keV x-rays can exit towards the spectrometer with minimal reabsorption. The scattered signal is collected by a high–efficiency Bragg spectrometer using a highly oriented pyrolytic graphite (HOPG) crystal[17] which is mounted at a 40° scattering angle in forward direction. For detection we use an x–ray framing camera with a 180 ps gate. The measured signal is read out by a CCD camera fiber coupled to the framing camera. We flat–fielded the spectrometer using bremsstrahlung emission from an aluminum plasma to account for reflectivity inhomogeneities of the HOPG crystal and the multichannel plate detector. Gold shields are used to block the direct line of sight of the spectrometer to the plasmas generated by the heater and the backlighter beams.

Fig. 2 shows the recorded scattering spectrum. For comparison, the source spectrum that was measured on a dedicated saran disk shot is plotted. In addition to the main Cl Ly-α line a red–shifted satellite is present. However, the down-shifted inelastically scattered signal recorded on the full target shot is much stronger than the naturally occurring He–like satellite in the source spectrum. In addition to the down–shifted plasmon signal a clear inelastically scattered, up–shifted signal is observed.

To quantify the temperature, synthetic scattering spectra were generated and fit to the experimental data. To model the spectra we applied the random phase approximation for the electron structure factor.[13] The source spectrum recorded on the Saran disk shot was used to define the instrument function. The best agreement between the measured scattering signal was obtained for $n_e = 1.8\times10^{23}$ cm^{-3} and an electron temperature of 18 eV (cf. Fig. 2).

In addition, in principle the ratio of the plasmon signal to the Rayleigh signal allows to infer the plasma temperature. The strength of the Rayleigh peak depends on the static ion-ion structure factor which increases with ion temperature. Here we use the screened one component plasma model[18] to calculate $S_{ii}(k)$ which has proven to yield the correct values for other systems.[1] However, for this experiment with beryllium we are not able to consistently model the spectrum, i.e, to obey the constraint $T_e = T_i$. If this constraint is removed, and T_i used as a fitting parameter, for $T_i = 6$ eV an excellent agreement between the synthetic spectrum and the experimental data is achieved (cf. Fig. 2). Recently, density functional calculations coupled to molecular-dynamics simulations have been developed which more accurately model $S_{ii}(k)$ for beryllium.[16] The discrepancy between these different

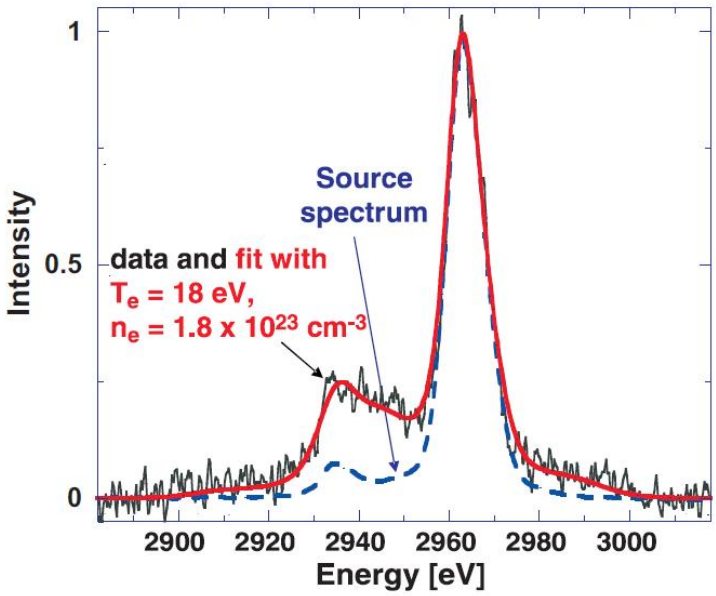

Figure 2. Measured x-ray Thomson scattering spectrum of isochorically heated beryllium. The synthetic spectrum (solid line), obtained with $n_e = 1.8 \times 10^{23}$ cm^{-3} and $T_e = 18$ eV, represents the best fit to the data. For comparison, the source spectrum recorded on a Saran disk shot is shown (dashed line) [reproduced from T. Döppner *et al.*, High Energy Density Physics **5**, 182 (2009)].

theoretical approaches highlights the importance of first principle methods like temperature measurement using the detailed balance relation to validate theoretical predictions.

The ratio of the plasmon signal to the Rayleigh peak is also sensitive to the ionization state Z_f. However, since we used T_i as a free parameter to fit the Rayleigh peak, for further analysis we have to make an assumption about the ionization state. We choose $Z_f = 2.3$, as reported for similar plasma conditions,[5] and in accordance with hydrodynamical simulations. From the electron density determined from the plasmon shift in the x-ray Thomson scattered spectrum this corresponds to a mass density of 1.17 g cm^{-3} which is about 2/3 of solid Be, suggesting that expansion of the Be has started before the x-ray probe arrives. This is in very good agreement with 1D radiation-hydrodynamical (HELIOS[19]) simulations which show some rarefaction at the rear surface of the Be foil at the time of the x-ray Thomson scattering measurement.[11]

3. DISCUSSION

The above described collective scattering experiment heated the beryllium foil just high enough that detailed balance, i.e. the asymmetry in up- and down–shifted plasmon signals, became quantitatively observable. To obtain a more prominent up-shifted plasmon signal, the Be foil has to be heated to higher temperatures. This can be achieved, for example, by increasing the energy in the backlighter beams and decreasing the Be foil thickness. However, certain restrictions have to be obeyed. For example, decreasing the target thickness will reduce the time window for the probing before the shock wave, launched by the heater beams, reaches the rear surface of the foil.

In addition, the observation of detailed balance will be most distinct, if the scattering geometry is very collective ($\alpha > 1.5$). Low scattering angles will allow for large α. However, scattering angles below 25° are difficult to implement because (i) the probe has to penetrate more material reducing the transmission, and (ii) shielding the detector from having a direct line of sight to the x-ray source becomes a problem. In addition the plasmon shift decreases for smaller scattering angles. For small values of k, i.e., large values of α, the plasmon shift $\hbar\omega_{res}$ can be calculated using the Bohm-Gross relation,[20,21] an analytical expansion of the dispersion

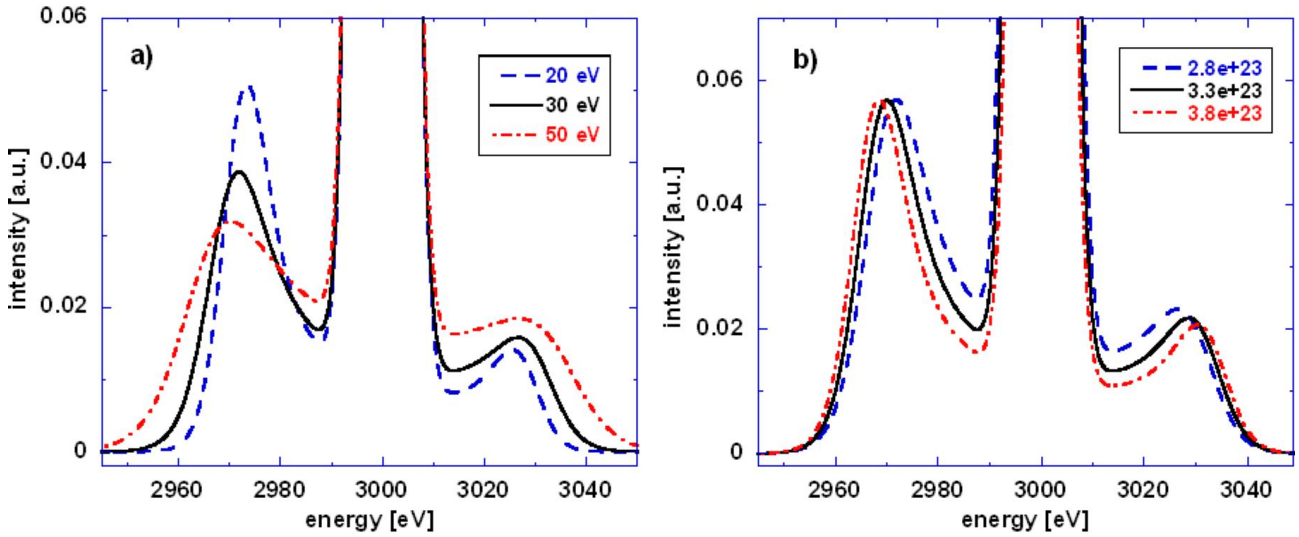

Figure 3. Simulated scattering spectra for varying temperature (left, $Z_f = 2.3$, $n_e = 2.8 \times 10^{23}$ cm^{-3} are fixed) and densities (right, in cm^{-3}, $T_e = 30$ eV and $\rho = 1.85$ g/cc are fixed). The spectra were calculated for a scattering angle of 30°, and assuming an instrument function with a FWHM of 8 eV.

relation

$$\omega_{res}^2 = \omega_p^2 + 3k^2 v_{th}^2 (1 + 0.088 n_e \Lambda^3) + \left(\frac{\hbar k^2}{2m_e}\right)^2 \tag{6}$$

where $v_{th} = \sqrt{k_B T/m_e}$ is the thermal velocity and $\Lambda_e = h/2\pi m_e k_B T$ is the thermal wavelength. The first term in Eq. 6 is the plasma frequency $\omega_p = (n_e e^2/\epsilon_o m_e)^{1/2}$ that is only dependent on the electron density, n_e. The second term represents the effect on propagation of the oscillations from thermal pressure.[20] For large temperatures this can be the dominant contribution to the resonance frequency in the scattering experiment. The third term in Eq. 6 includes degeneracy effects from Fermi pressure,[22] and the last term is the quantum shift, calculated from the Compton energy.

To explore how higher temperatures affect plasmon signatures in Thomson scattering spectra, new methods to isochorically and uniformly heat matter have to be explored. For example, very recently intense ultra-short FEL laser pulses at 92 eV were utilized to induce saturable absorption in aluminum.[23] This property can be exploited to heat macroscopic bulk samples with great spatial homogeneity. We propose a new experiment that utilizes fast electrons, generated by powerful short pulse lasers, to isochorically heat beryllium. Infrared picosecond laser pulses with intensities above 10^{17} W/cm^2, upon impact on solid targets, accelerate electrons to MeV energies. Conversion efficiencies on order of 30% into fast electrons have been inferred.[24] kJ-class lasers are able to heat samples sizes of order 200 microns to temperatures of several 100 eV.

We are interested in heating beryllium up to about 50 eV, a regime which is relevant for inertial confinement fusion on the National Ignition Facility.[25] Fig. 3 shows how the plasmon signals change with temperature (left) and electron density (right). For clarity we simulated the spectra neglecting the Cl Ly-α satellite, down-shifted by about 30 eV from the main Cl Ly-α line (cf. source spectrum in Fig. 2). Its nearly elastically scattered signal clearly interferes with the down-shifted plasmon signal. However, its strength depends on the correct knowledge of the structure factor $S_{ii}(k)$ (cf. Eq. 5). Experiments and recent density functional calculations coupled to molecular dynamics simulations (MD-DFT)[16] give evidence that the simulated spectra presented in this contribution for berylliium overestimate the weight of the Rayleigh feature by about a factor of 2.

For the simulated spectra in Fig. 3 we assumed a Gaussian instrument function with a width at half maximum of 8 eV. A scattering angle of 30° is used that allows to obtain collectivity parameters up to $\alpha \leq 1.8$. Fig. 3a shows the effect of increasing temperature at constant density. We assumed Be at solid density, $\rho = 1.85$ g cm^{-3}, and ionization of $Z_f = 2.3$ as observed in previous experiments at comparable plasma conditions,[5] yielding an

electron density of $n_e = 2.8 \times 10^{23}$ cm^{-3}. The spectra are normalized to the strength of the Rayleigh feature, which also depends on temperature. The plasmon signal show two distinct trends with rising temperature. (i) The relative strength of the up–shifted plasmon feature increases according to the detailed balance relation (cf. Eq. 4). (ii) The plasmon shift $\hbar\omega_{res}$ clearly increases due to the second term in Eq. 6. Note, that this also affects the asymmetry of the up-and down shifted plasmons (cf. Eq. 4). In addition to that, the width of the plasmon signals clearly increases with rising temperatures. This is due to fact that at $T_e = 50$ eV the scattering is not purely collective anymore. α depends on T_e through the screening length λ_{scr}, and decreases from 1.82 to 1.25 while the temperature rises from 20 eV to 50 eV.

Fig. 3b shows the effect of increasing electron density at constant electron temperature $T_e = 30$ eV. We again assumed constant mass density, $\rho = 1.85$ g cm^{-3}. Here, n_e is varied between 2.8 and 3.8×10^{23} cm^{-3} by changing the ionization from $Z_f = 2.3$ to 3.1, respectively. The simulated spectra are normalized to the down–shifted plasmon signal. The plasmon signals clearly show larger shifts $\hbar\omega_{res}$ with increasing electron density which is due to the first term in Eq. 6, i.e. a larger plasma frequency ω_p. In addition, with larger plasmon shifts the asymmetry increases of up– and down–shifted plasmons according to the detailed balance relation increases (cf. Eq. 4). α depends on n_e through the screening length. Hence α increase with electron density, here from 1.57 to 1.79 when varying n_e from 2.8 to 3.8×10^{23} cm^{-3}.

To simplify the discussion, we kept either T_e or n_e constant in Fig. 3. In reality, both quantities will change at the same time. Rising temperatures will cause higher ionization Z_f and thus higher electron densities. Previous experiments on isochorically heated Be in the non-collective scattering regime measured that Z_f increased from 2.3 to 2.7 for electron temperatures between 2 eV and 53 eV,[4] i.e. temperature rises much faster than ionization. Hence even though ionization and electron density are going up, α goes down because of large T_e change, having the major impact on the screening length. Thus T_e can become a major factor that governs the nature of the scattering experiment.

This has to be taken into account when designing an experiment that has to be strictly collective, for example to investigate the influence of collisions in warm dense matter. For the case of solid density beryllium, probed with a 3 keV x-ray line source as described in this contribution, the temperature has to be below 30 eV and the scattering angle has to kept at 30° to achieve $\alpha = 1.7$ or above, to be in a purely collective scattering regime.

4. CONCLUSION

We described an experiment that isochorically heated a 250 μm thick Be foil using Ag L–shell radiation. In the collective scattering regime up– and down–shifted plasmon signals were simultaneously measured. From detailed balance an electron temperature of 18 eV with an error of 20% could be inferred. Assuming a mean charge state of $Z = 2.3$, the mass density was deduced to be 1.2 ± 0.2 g cm^{-3}, which is 30% below solid beryllium, indicating rarefaction at the rear surface which is in accordance with 1D hydrodynamical simulations. Temperature measurement through detailed balance is based on first principles, and will be important to validate theoretical models that calculate ion-ion structure factors.

ACKNOWLEDGMENTS

This work was performed under the auspices of the U.S. Department of Energy by the Lawrence Livermore National Laboratory, through the Institute for Laser Science and Applications, under contract DE-AC52-07NA27344. The authors also acknowledge support from Laboratory Directed Research and Development Grants No. 08-LW-004 and 08-ERI-002.

REFERENCES

[1] Kritcher, A.L., Neumayer, P., Castor, J., Döppner, T., Falcone, R.W., Landen, O.L., Lee, H.J., Lee, R.W., Morse, E., Ng, A., Pollaine, S., Price, D., and Glenzer, S.H., "Ultrafast x-ray thomson scattering of shock-compressed matter," *Science* **322**, 69 (2008).

[2] Lindl, J.D., Amendt, P., Berger, R.L., Glendinning, S.G., Glenzer, S.H., Haan, S.W., Kauffman, R.L., Landen, O.L., and Suter, L.J., "The physics basis for ignition using indirect-drive targets on the national ignition facility," *Phys. Plasmas* **11**(2), 339 (2004).

[3] Glenzer, S.H. and Redmer, R., "X-ray Thomson Scattering," *Rev. Mod. Phys., in print* (2009).

[4] Glenzer, S.H., Gregori, G., Lee, R.W., Rogers, F.J., Pollaine, S.W., and Landen, O.L., "Demonstration of spectrally resolved x-ray scattering in dense plasmas," *Phys. Rev. Lett.* **90**(17), 175002 (2003).

[5] Glenzer, S.H., Landen, O.L., Neumayer, P., Lee, R.W., Widmann, K., Pollaine, S.W., Wallace, R.J., Gregori, G., Höll, A., Bornath, T., Thiele, R., Schwarz, V., Kraeft, W.D., and Redmer, R., "Observations of plasmons in warm dense matter," *Phys. Rev. Lett.* **98**(6), 065002 (2007).

[6] Barbrel, B., Koenig, M., Benuzzi-Mounaix, A., Brambrink, E., Brown, C.R.D., Gericke, D.O., Nagler, B., le Gloahec, M.R., Riley, D., Spindloe, C., Vinko, S.M., Vorberger, J., Wark, J., Wünsch, K., and Gregori, G., "Measurement of short-range correlations in shock-compressed plastic by short-pulse x-ray scattering," *Phys. Rev. Lett.* **102**, 165004 (2009).

[7] Fäustlin, R.R., Toleikis, S., Bornath, T., Döppner, T., Düsterer, S., Förster, E., Fortmann, C., Glenzer, S.H., Göde, S., Gregori, G., Irsig, R., Laarmann, T., Lee, H.J., Li, B., Meiwes-Broer, K.-H., Mithen, J., Przystawik, A., Redlin, H., Redmer, R., Reinholz, H., Röpke, G., Tavella, F., Thiele, R., Tiggesbäumker, J., Uschmann, I., Zastrau, U., and Tschentscher, T., "Soft X-Ray Thomson Scattering in Warm Dense Hydrogen at FLASH," *SPIE Proceedings, Optics and Photonics Conference, San Diego 2009* (2009).

[8] Lee, H.J., Neumayer, P., Castor, J., Döppner, T., Falcone, R.W., Fortmann, C., Hammel, B.A., Kritcher, A.L., Landen, O.L., Lee, R.W., Meyerhofer, D.D., Munro, D.H., Redmer, R., Regan, S.P., Weber, S., and Glenzer, S.H., "X-ray Thomson-Scattering Measurements of Density and Temperature in Shock-Compressed Beryllium," *Phys. Rev. Lett.* **102**, 115001 (2009).

[9] Pines, D. and Nozieres, P., [*The Theory of Quantum Fluids*], Addison-Wesley, Redwood City, CA (1990).

[10] Höll, A., Bornath, T., Cao, L., Döppner, T., Düsterer, S., Förster, E., Fortmann, C., Glenzer, S.H., Gregori, G., Laarmann, T., Meiwes-Broer, K.-H., Przystawik, A., Radcliffe, P., Redmer, R., Reinholz, H., Röpke, G., Thiele, R., Tiggesbäumker, J., Toleikis, S., Truong, N.X., Tschentscher, T., Uschmann, I., and Zastrau, U., "Thomson scattering from near-solid density plasmas using soft x-ray free electron lasers," *High Energy Density Physics* **3**(3), 120 (2007).

[11] Döppner, T., Landen, O.L., Lee, H.J., Neumayer, P., Regan, S.P., and Glenzer, S.H., "Temperature measurement through detailed balance in x-ray Thomson scattering," *High Energy Density Physics* **5**, 182 (2009).

[12] Chihara, J., "Interaction of photons with plasmas and liquid metals-photoabsorption and scattering," *Journal of Physics-Condensed Matter* **12**(3), 231 (2000).

[13] Gregori, G., Glenzer, S.H., Rozmus, W., Lee, R.W., and Landen, O.L., "Theoretical model of x-ray scattering as a dense matter probe," *Physical Review E* **67**(2), 026412 (2003).

[14] Wünsch, K., Vorberger, J., and Gericke, D.O., "Ion structure in warm dense matter: Benchmarking solutions of hypernetted-chain equations by first-principle simulations," *Phys. Rev. E* **79**, 010201(R) (2009).

[15] Gregori, G. and Gericke, D.O., "Low frequency structural dynamics of warm dense matter," *Physics of Plasmas* **16**, 056306 (2009).

[16] Gericke, D.O., Vorberger, J., Wünsch, K., Neumayer, P., Döppner, T., Lee, H.J., Kritcher, A.L., Landen, O.L., and Glenzer, S.H., "Structure of warm dense beryllium applied to x-ray Thomson scattering," *submitted to Phys. Rev. Lett.* (2009).

[17] Pak, A., Gregori, G., Knight, J., Campbell, K., Price, D., Hammel, B.A., Landen, O.L., and Glenzer, S.H., "X-ray line measurements with high efficiency Bragg crystals," *Review of Scientific Instruments* **75**(10), 3747 (2004).

[18] Gregori, G., Ravasio, A., Höll, A., Glenzer, S.H., and Rose, S.J., "Analytical derivation of the static structure factor in strongly-coupled non-equilibrium plasmas for x-ray scattering studies," *High Energy Density Physics* **3**(3), 99 (2007).

[19] MacFarlane, J.J., Golovkin, I.E., and Woodruff, P.R., "HELIOS-CR - A 1-D radiation-magneto-hydrodynamics code with inline atomic kinetics modeling," *J. Quant. Spectrosc. RA* **99**(1-3), 381 (2006).

[20] Bohm, D. and Gross, E.P., "Theory of plasma oscillations.a. origin of medium-like behavior," *Physical Review* **75**(12), 1851 (1949).

[21] Thiele, R., Bornath, T., Fortmann, C., Höll, A., Redmer, R., Reinholz, H., Röpke, G., Wierling, A., Glenzer, S.H., and Gregori, G., "Plasmon resonance in warm dense matter," *Phys. Rev. E* **78**, 026411 (2008).

[22] Zimmermann, R., Kilimann, K., Kraeft, W.D., Kremp, D., and Röpke, G., "Dynamical screening and self-energy of excitons in electron-hole plasma," *Physica Status Solidi B-Basic Solid State Physics* **90**(1), 175 (1978).

[23] Nagler, B., Zastrau, U., Fäustlin, R.R., Vinko, S.M. et al., "Turning solid aluminium transparent by intense soft X-ray photoionization," *Nature Physics* , doi: 10.1038/nphys1341 (2009).

[24] Nilson, P.M., Theobald, W., Myatt, J.F., Stoeckl, C., Storm, M., Zuegel, J.D., Betti, R., Meyerhofer, D.D., and Sangster, T.C., "Bulk heating of solid-density plasmas during high-intensity-laser plasma interactions," *Phys. Rev. E* **79**, 016406 (2009).

[25] Hammel, B.A., Edwards, M.J., Haan, S.W., Marinak, M.M., Patel, M., Robey, H., and Salmonson, J., "Simulations of high-mode Rayleigh-Taylor growth in NIF ignition capsules," *Journal of Physics: Conference Series* **112**, 022007 (2007).